Higher-order correction terms to the nonlinear amplification or absorption, the nonlinear refractive index, and the intrapulse Raman scattering

Ivan M. Uzunov and Todor N. Arabadzhiev *

Department of Applied Physics, Faculty of Applied Mathematics and Informatics, Technical University of Sofia, 8 Kl. Ohridski Blvd., Sofia 1000, Bulgaria

(Received 14 October 2020; accepted 19 January 2021; published 9 February 2021)

In this paper we have investigated through the numerical solution of the basic equation as well as through the dynamic model the influence of higher-order correction terms to the nonlinear amplification (absorption) and to the nonlinear refractive index on the self-frequency shift of Raman dissipative solitons. We have found a nonlinear dependence of the self-frequency shift of Raman dissipative solitons on the parameter describing intrapulse Raman scattering in the presence of the saturation of the nonlinear gain. With the increase of the absolute value of the saturation of the nonlinear gain, the maximum absolute value of the frequency shift decreases and its position moves to larger values of the parameter describing intrapulse Raman scattering. The increase in the value of the nonlinear gain leads to an increase in the maximum absolute value of the frequency shift, without changing its position. We have also observed the nonlinear dependence of the absolute value of the frequency shift on the parameter describing intrapulse Raman scattering in the presence of higher-order correction term to the nonlinear refractive index. The discovered nonlinear dependence of the self-frequency shift on the value of the saturation of the nonlinear gain as well as on the higher-order correction term to the nonlinear refractive index can be used for the better understanding and control of the spectral characteristics of Raman dissipative solitons. The dynamic model correctly describes all the features of the observed phenomena.

DOI: 10.1103/PhysRevE.103.022208

I. INTRODUCTION

In optics the complex cubic-quintic Ginzburg–Landau equation (CCQGLE) and the complex cubic Ginzburg–Landau equation (CCGLE) have been used to describe a passive mode-locked solid state and fiber lasers [1–3] as well as wave propagation in nonlinear optical fibers with gain and spectral filtering [4–6]. The known exact solutions as well as the numerical solutions of the CCQGLE have been reviewed in Refs. [7,8]. Some example solutions in the negative dispersion region worth mentioning are localized stationary solutions as well as pulsating solutions: plain pulsating, creeping, and erupting (exploding) solutions [9,10].

Finite-dimensional dynamic models have been used for determining the exact solutions of the CCQGLE [11–15] and their stability [16,17] as well as for the dynamic analysis of the solutions of the CCQGLE. In the last case finite-dimensional dynamic models have been derived through the soliton perturbation theory [5], the method of moments [18–21], and the variation method in Ref. [22].

For the study of ultrashort optical pulses, it is necessary to include higher-order effects (HOE): third order of dispersion (TOD), self-steepening (SS), and intrapulse Raman scattering (IRS) [5,6,23–25]. The stimulated Raman self-scattering of femtosecond optical solitons has been experimentally discovered in Refs. [26,27]. This effect is also called intrapulse stimulated Raman scattering, or often intrapulse Raman scattering [5,6,28]. In this regime of stimulated Raman scattering, the spectrum of a high-power short laser pulse proves to be so broad that it covers the band of Raman resonances of the medium. In this case, the Stokes spectral component of the field shifted by the frequency of molecular vibrations is contained within the pump pulse itself. The amplification of low-frequency Stokes components in the field of high-frequency anti-Stokes spectral components of the same soliton pulse results in a continuous shift of its spectrum known as soliton Raman self-frequency shift [6]. This effect plays an important role in studies of a supercontinuum generation [29,30].

Attention has been paid to the investigation of the influence of HOE on the exploding solutions numerically [31,32] and analytically [33]. The transition of erupting solutions under the influence of SS to fixed-shape solutions has been studied in Ref. [34]. The appearance of a periodic erupting solution has been observed under the influence of IRS and has been related to the sequence of period halving and period doubling bifurcations controlled by the IRS parameter [35]. The influence of noise (additive and multiplicative), and HOE on exploding solutions has been studied [36].

The influence of HOE on the localized stationary solutions (dissipative solitons) as well as on the plain pulsating solutions is of great theoretical and practical importance. An exact solution of the CCQGLE perturbed with HOE has been identified which requires a specific relation between the physical parameters and the parameters of the solution [23]. A finite-dimensional dynamic system for the amplitude and frequency of the soliton solution has been derived [37,38]. The analysis

* tna@tu-sofia.bg

of its stationary solutions as well as their stability has shown that narrow-band filtering and nonlinear gain can control the self-frequency shift due to the IRS of ultrashort optical solitons [37,38]. Thanks to the further analysis of the dynamic system of [37,38] we have found the Poincaré-Andronov-Hopf bifurcation with respect to the parameter describing IRS [39]. In order to describe the influence of the saturation of the nonlinear gain as well as the influence of TOD and SS on this bifurcation, a dynamic system describing the spatial evolution of all soliton parameters (amplitude, frequency, time position, and phase) has been derived and shortly presented in Refs. [40–42]. It has been shown that TOD and SS can lead to a reduction in the time shift of the pulse [40,42]. The existence of short high-amplitude dissipative solitons in the presence of IRS has been found [42] using the dynamic system of Refs. [40–42]. It has also been shown that for the singularity in the solution of the CCQGLE when the saturation of the nonlinear gain tends to zero [13] (see parameter μ when it is negative below), no more exists in the presence of IRS [42]. The perturbation approach using as initial ansatz the form closer to the exact solution of the CCGLE for the analysis of perturbed with HOE CCGLE has been presented in Ref. [43]. Using the method of momentum [18] we have developed the finite degree of a freedom model which takes into account the independent evolution of the width and chirp of the pulse for the analysis of the influence of HOE on the solutions of the CCQGLE in the anomalous dispersion regime [41,44] (see also Ref. [45]). The transformation of the single-spike dissipative solitons with extreme spikes of CCQGLE into dissipative solitons have been found in Ref. [46]. There it was found numerically as well as by the model [44] that the amplitude of the Raman dissipative solitons decreases, while the absolute value of the self-frequency shift decreases with the increase of the value of the IRS. In a recent study the role of IRS as a feedback mechanism for the existence of stable propagating dissipative solitons with uniquely determined velocity in CCGLE has been studied through a semianalytical approach [47]. It has been shown that the limit of the vanishing magnitude of the IRS coefficient is singular. In Ref. [48] the influence of IRS, SS, and TOD on the solutions of the CCQGLE has been studied by means of bifurcation analysis of the dynamical model (DM) proposed in Ref. [44]. The following types of transformations have been identified: (a) from chaotic into two-periodic solution; (b) from two periodic into a limit cycle; and (c) from a limit cycle into a stationary solution under the influence of IRS. Interaction between all higher-order effects has been studied [48]. Following the idea of Ref. [48] in Ref. [49] we have studied numerically the influence of IRS and self-steepening on the period-2 pulsating solution of the CCQGLE. A cascade of transformations of the numeric solutions under the influence of SS has been reported, which includes the existence of: period-1 solutions, chaotic solutions, period-doubling transformations, and others. It has been shown that by increasing the IRS parameter, the period-4 pulsating solution related to the SS can be successfully transformed into a period-2, period-1 pulsating solutions and, finally, into a stationary solution [49]. It has been mentioned [48] and reported in Ref. [50] that the obtained numerical results of Ref. [47] can be described very well by the dynamic model of Ref. [44].

We present here a study of the localized stationary solitonlike solutions of the perturbed CCGLE and CCQGLE with the terms responsible for the IRS. As the solitonlike solutions of CCGLE and CCQGLE are usually called dissipative solitons, we may formulate our aim as the study of the self-frequency shift of the Raman dissipative solitons (RDS). Our aim is to study the influence of the nonlinear gain, higher-order correction terms to the nonlinear amplification (absorption) and to the nonlinear refractive index on the self-frequency shift of RDS. In order to accomplish this, we have solved numerically the basic equation with the Agrawal's split-step Fourier method with two iterations and applied the dynamic model with finite degrees of freedom obtained with the method of moments [44]. A detailed comparison of the results obtained by these two methods has been presented and analyzed.

The paper is organized as follows: First, the physical meaning and application of the CCQGLE perturbed with higher-order effects are presented in Sec. II. In Sec. III we introduce the finite-dimensional dynamic model derived in Ref. [44] as well as the approximate fixed points of the model. In Sec. IV we study the IRS in the presence of nonlinear gain. We fix the value of the parameter describing IRS and change the parameter describing the nonlinear gain. The presented results show that the self-frequency shift of the RDS increases with the increase of the value of the nonlinear gain. In Sec. V we present our results concerning the influence of higher-order correction term to the nonlinear amplification (absorption) on the self-frequency shift of the RDS. We have found a nonlinear dependence of the absolute value of the self-frequency shift of RDS on the parameter describing IRS in the presence of the saturation of the nonlinear gain. With the increase of the absolute value of the saturation of the nonlinear gain the maximum of the absolute value of the frequency shift decreases and its position moves to larger values of the parameter describing IRS. In Sec. VI we present our results concerning the influence of higher-order correction terms to the nonlinear refractive index on the self-frequency shift of the RDS. Here we present our findings for the nonlinear dependence of the absolute value of the frequency shift on the γ in the presence of the higher-order correction term to the nonlinear refractive index. Our discussion of the applicability of the dynamic model [44] is presented in Sec. VII. Finally, we make our conclusions in Sec. VIII.

II. NUMERICAL CALCULATION OF THE BASIC EQUATION

The dynamic behavior is described by the following CCQGLE perturbed by IRS [1–6]:

$$i\frac{\partial U}{\partial x}+\frac{1}{2}\frac{\partial^2 U}{\partial t^2}+|U|^2U = i\delta U+i\beta\frac{\partial^2 U}{\partial t^2}+i\varepsilon|U|^2U-\nu|U|^4U+i\mu|U|^4U +\gamma U\frac{\partial}{\partial t}(|U|^2)\,, \tag{1}$$

where U is the normalized envelope of the electric field, t and x are the retarded time and the normalized propagation distance, δ is the linear loss-gain coefficient, β describes the

spectral filtering (gain dispersion), ε is the nonlinear gain or absorption coefficient [14–16] (the nonlinear gain arises from the saturable absorption), μ, is the higher-order correction term to the nonlinear amplification (absorption) [14–16] (if negative, it accounts for the saturation of the nonlinear gain [10,19]), ν is the higher-order correction term to the nonlinear refractive index [14–16] (if negative, it corresponds to the saturation of the nonlinear refraction index [10]). In this equation we have implied that the group-velocity dispersion is anomalous. Parameter γ takes into account the effect of the IRS in the simplest quasi-instantaneous description. In this case there has been applied a linear approximation to the frequency-domain Raman response function [51–54]. Such a description of the IRS is valid for pulses shorter than 1 ps but wide enough to contain many optical cycles (pulse width $\geqslant$100 fs) [6]. Equation (1) considers a frame of reference moving with the pulse. Equation (1) is basically a phenomenological model, but it has proved to be a good qualitative model for the real mode-locked lasers. It has been proposed as a master equation for solid-state lasers with fast saturable absorber [1–3] as well as for the mode-locked fiber lasers [55,56]. The relations between the physical parameters describing a ring fiber laser mode locking through nonlinear polarization rotation and the coefficients of CCQGLE have been derived in Ref. [57].

For the numerical solution of Eq. (1), we have used Agrawal's split-step Fourier method with two iterations [58,59]. The numerical parameters for this calculation are as follows: time resolution: 0.0002–0.002 44, number of samples: 2^{15}–2^{17}, a constant propagation step (but case dependent)—with size between 10^{-3} and 10^{-5} or adaptive step size. The following numerical quantities have been calculated numerically solving Eq. (1): mean frequency: $\omega(x) = \int_{-\infty}^{+\infty} \omega |U(x,\omega)|^2 d\omega / \int_{-\infty}^{+\infty} |U(x,\omega)|^2 d\omega$, peak amplitude: $\eta(x) = \max |U(x,t)|, \forall t$, velocity: $\mathrm{v}(x) = (\int_{-\infty}^{+\infty} t|U(x,t)|^2 dt / \int_{-\infty}^{+\infty} |U(x,t)|^2 dt)/x$ and identical to the model (3) time width: $\sigma(x) = (\tau(x)/\tau(0))/\eta(0)$, where $\tau(x) = \int_{-\infty}^{+\infty} |U(x,t)|^2/\eta(x)^2 dt$. We also use the quantity full width at half maximum: FWHM $= 2.6339\sigma(x)$. Because of the internal properties of the fast Fourier transformation, the initial condition used for the direct calculation of (1) contrary to (2) has a negative phase sign: $U(0,t) = \eta \sec h[\eta t] \exp[-i\omega t]$. That is why, in the results, the sign of the frequency obtained by (3) is the same as the frequency sign obtained by Eq. (1) which corresponds to the physical reality.

III. DYNAMIC MODEL AND APPROXIMATED FIXED POINTS

To derive the dynamic system, we use the trial function in the following form [18,19,20,44]:

$$U(x,t) = \eta(x)\mathrm{sech}\left[\frac{t-k(x)}{\sigma(x)}\right]\exp[i\omega(x)(t-k(x)) + ic(x)(t-k(x))^2], \tag{2}$$

where $\eta(x)$, $\sigma(x)$, and $k(x)$ are, respectively, the amplitude, width, and position of the pulse maximum, $\omega(x)$ is the frequency, and $c(x)$ is the chirp parameter. Applying the method of moments of Ref. [18] we obtain the following set of ordinary differential equations for the parameters $\eta(x)$, $\sigma(x)$, $k(x)$, $\omega(x)$, and $c(x)$ [44]:

$$\begin{aligned}
\frac{d\eta}{dx} &= (\delta - c)\eta + \beta\left(\frac{\eta(-60 - 5\pi^2 + 3\pi^4 c^2\sigma^4)}{15\pi^2\sigma^2} - \eta\omega^2\right) \\
&\quad + \varepsilon\frac{2(3+\pi^2)}{3\pi^2}\eta^3 + \mu\frac{2}{15}\left(4 + \frac{15}{\pi^2}\right)\eta^5 \\
\frac{d\omega}{dx} &= -4\beta\frac{(1+\pi^2 c^2\sigma^4)\omega}{3\sigma^2} + \frac{8}{15}\gamma\frac{\eta^2}{\sigma^2}, \\
\frac{dk}{dx} &= \omega - \frac{2\pi^2}{3}\beta c\omega\sigma^2 \\
\frac{d\sigma}{dx} &= 2c\sigma + \beta\left(\frac{8}{\pi^2\sigma} - \frac{16}{15}\pi^2 c^2\sigma^3\right) - \frac{4}{\pi^2}\varepsilon\sigma\eta^2 - \frac{4}{\pi^2}\mu\sigma\eta^4 \\
\frac{dc}{dx} &= \left(-2c^2 + \frac{2}{\pi^2\sigma^4} - \frac{2\eta^2}{\pi^2\sigma^2}\right) - \beta\frac{4(3+\pi^2)c}{3\pi^2\sigma^2} - \nu\frac{32\eta^4}{15\pi^2\sigma^2}
\end{aligned} \tag{3}$$

Dynamic system (3) allows the study of the influence of the IRS on the localized solutions of the CCQGLE. We also use the quantity full width at half maximum: FWHM $= 2.6339\sigma(x)$. System (3) for the cases of $\delta \neq 0$, $\nu \neq 0$, has been first derived and studied in Ref. [18]. The essential point in the derivation of this equation is the relation between the width and chirp of the pulse [18]. A simpler form of Eq. (3) has been studied where $\delta \neq 0$, $\beta \neq 0$, $\nu \neq 0$, $\varepsilon \neq 0$, $\mu \neq 0$ with $\gamma = 0$ [19,20]. The position $k(x)$ is not involved in the first, second, fourth, and fifth equations, so it will not be involved in the search for the fixed points of DM (3). It has been shown that at $\beta > 0$ and for $x- > \infty$, the frequency ω tends to zero and the pulse position k tends to a constant value which has allowed the authors to obtain a three-dimensional system of ordinary differential equations for the amplitude $\eta(x)$, width $\sigma(x)$, and chirp of the pulse $c(x)$. The velocity v corresponds to $k(x_{\max})/x_{\max}$ while the FWHM corresponds to $2\ln(2+\sqrt{3})\sigma(x_{\max})$. It has been found that there exists a correspondence between the attractors of the model and the localized solutions of the CCGLE, namely, that the stationary solutions of the CCGLE correspond to fixed points, while the pulsating solutions are related to stable limit cycles [19,20]. However, it is well known that the IRS leads to changes in the pulse frequency, pulse shape, and pulse spectrum. So, the frequency $\omega(x)$ becomes a function of the distance of propagation and should not be neglected.

In the case of the CCGLE perturbed with IRS, we have found approximated fixed points for three of the parameters in dynamic model (3): amplitude, frequency, and width. To get these fixed points we have assumed that the chirp is zero and have neglected the fifth equation for the chirp. It has turned out that this assumption is not an obstacle for obtaining useful results. We have introduced the pulse energy as $Q = \eta^2\sigma$. Solving the reduced system of three equations for identifying the stationary solutions (η, ω, σ), we have found four different fixed points of which only one has a physical meaning:

$$\begin{aligned}
&Q = (2\sqrt{10}\beta)/(\varepsilon q); \quad \eta = (2\sqrt{5\beta})/(q\sqrt{\varepsilon}); \\
&\omega = (5\beta\varepsilon^2 + p)/(8\beta\gamma\varepsilon); \quad \sigma = q/\sqrt{10};, \quad \text{where} \\
&p = \sqrt{\beta\varepsilon^2(64\gamma^2\delta + 25\beta\varepsilon^2)}; \quad q = \sqrt{(-5\beta\varepsilon^2 + p)/\delta\varepsilon^2}.
\end{aligned} \tag{4}$$

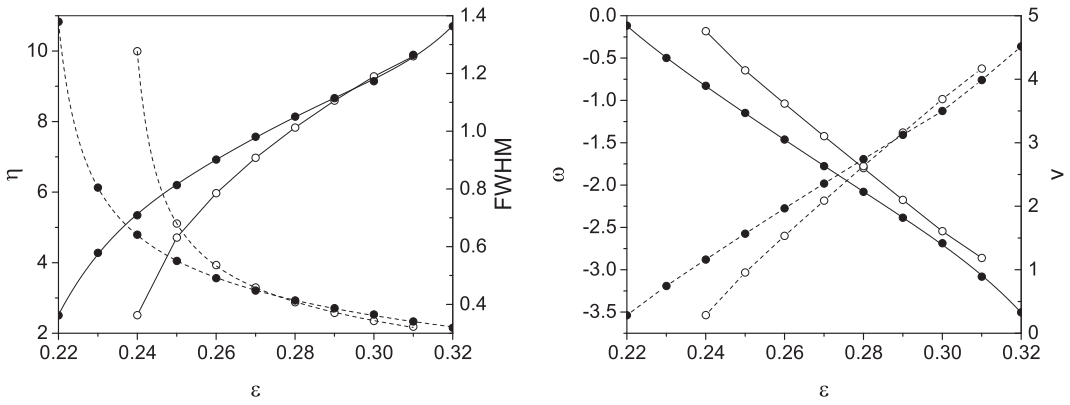

(a) (b)

FIG. 1. Results obtained by direct numerical solution of (1) (solid circles) and the numerical solution of DM (3) (empty circles) for (a) the peak amplitude (solid lines) and FWHM (dashed lines); (b) mean frequency (solid lines) and velocity (dashed lines) as functions of $\varepsilon \subset [0.22; 0.32]$ at parameters $\delta = -0.012$; $\beta = 0.6$; $\gamma = 0.05$; $\eta(0) = 10$; $\sigma(0) = 1/\eta(0)$; $c(0) = 0; \omega(0) = 0$. The propagation distance is $x_{\max} = 200$.

It turned out that this fixed point correctly describes our numerical observations in the case of the CCGLE perturbed with IRS.

The principal question for the applicability of dynamic model (3) is whether during its propagation the numerical localized solutions are close to the sech-like form of Eq. (2). In this work we focus our attention on solitonlike numerical solutions, so we have chosen a set of values for the physical parameters used in the solving of Eq. (1) which will satisfy the requirements for achieving those solutions. In the process of our study this question of the preservation of the time shape of numerical solutions will be analyzed. The numerical solution of DM (3) presented here has been obtained by means of WOLFRAM MATHEMATICA [60] and MATLAB.

IV. CCGLE: THE INFLUENCE OF THE NONLINEAR GAIN ON THE SELF-FREQUENCY SHIFT

In nonlinear optics the influence of bandwidth-limited amplification characterized by δ, β on the IRS characterized by γ has been in the focus of some earlier studies [61–65]. It has been shown that in the presence of bandwidth-limited amplification, the soliton self-frequency shift due to the IRS decreases. It is well known that the parameter ε which describes the nonlinear gain of absorption plays a key role in the analysis of the properties of the solutions of CCGLE [14–16]. It has been shown that using narrow-band filtering and nonlinear gain, there can be achieved stable soliton propagation over long distances in the presence of IRS [38]. In order to describe the properties of the self-frequency shift of RDS in the perturbed with IRS CCGLE, we need two dependencies. The first one is the dependence of the parameters describing the RDS on ε for fixed γ and the second one, the dependence of the parameters describing the RDS on γ for fixed ε. We study here the first one, namely the influence of ε on all the parameters describing the RDS for fixed δ, β, and γ. The following values of the physical parameters have been used:, $\delta = -0.012$, $\beta = 0.6$, $\varepsilon = 0.3$ $\mu = 0$, $\nu = 0$. The important question is how to choose the values of the physical parameters. It is well known from the soliton perturbation theory that the soliton is stable provided that $\delta > 0$ and $\varepsilon < \beta/2$ [13,14]. The relation between β and ε ("curve S"), namely, $\varepsilon_S = \beta \frac{3\sqrt{1+4\beta^2}-1}{4+18\beta^2}$ on the plane (β, ε) divides it in such a way that in order to get "solutions with fixed amplitudes" we should have values of $\delta > 0$ below curve S and $\delta < 0$ above it [12,14]. On this line the solution with fixed amplitude becomes singular (its amplitude tends to infinity, while the width vanishes). In the case of $\beta \ll 1$ the $\beta \approx 2\varepsilon$ [12,14]. In the case of $\delta = 0$ the solutions on the curve S are "solutions with arbitrary amplitude" [12,14]. In our case $\beta = 0.6$ so $\varepsilon_S = 0.21$, and as $\varepsilon = 0.3 > \varepsilon_S$ and $\delta = -0.012$ is small and $d = 0.4$ what we get is slightly above the curve S so we could expect a solution with fixed amplitude, which, however, is close to the curve S, or to the solutions with arbitrary amplitudes [12,14].

Applying our dynamical model (3) we have established that for fixed values of δ, β, and parameter γ which characterizes IRS, by increasing the value of the nonlinear gain ε, the values of the amplitude and frequency of the stationary pulses also increase, so the self-frequency shift of the RDS is increased. These model predictions are verified in Fig. 1 below where the results from the numerical solution of the basic Eq. (1) are compared with the results of our model given in Eq. (3).

The numerical region for the change of the parameters describing the nonlinear gain $\varepsilon \in [0.22, 0.32]$ is chosen in the following way. After the numerical calculation of Eq. (1) we have found that for values of $\varepsilon < 0.22$, the numerical solutions are unstable ones: the amplitudes decrease and finally disappear. Next, for values of $\varepsilon > 0.32$, we have not obtained a stationary solution. For the calculation of the cases of $\varepsilon = 0.31, 0.32$ a step size of order 10^{-5} has been used. Figure 1 shows two ways of calculation: (a) direct numerical solution of Eq. (1); and (b) numerical solution by means of the dynamic model (3). As can be seen in Fig. 1, if we increase the value of the nonlinear gain ε, the values of the amplitude [Fig. 1(a)] and frequency [Fig. 1(b)] of the RDS also increase. Moreover, the pulse width decreases [Fig. 1(a)] while the velocity of the solutions [Fig. 1(b)] increases [Fig. 2(a)].

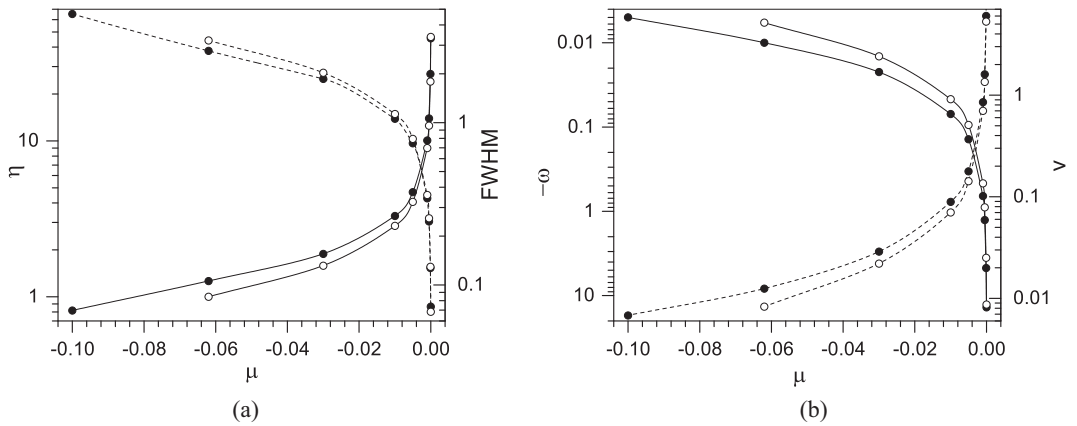

FIG. 2. Results obtained by direct numerical solution of (1) (solid circles) and the numerical solution of DM (3) (empty circles) for (a) the peak amplitude (solid lines) and FWHM (dashed lines); (b) mean frequency (solid lines) and velocity (dashed lines) as functions of $\mu \subset [-0.1; 0]$ (the ordinates are logarithmic) at parameters $\delta = -0.012$; $\beta = 0.6$; $\varepsilon = 0.3$; $\gamma = 0.01$. The initial condition is $\eta(0) = 1$; $\sigma(0) = 1/\eta(0)$; $c(0) = 0; \omega(0) = 0$.

From these results we can draw the conclusion that the self-frequency shift of the RDS increases with the increase of the value of the nonlinear gain ε. The pulse amplitude increases and its width decreases, i.e., solutions compress. Figure 1 represents the dynamic model (3) and correctly describes all the observed dependencies.

The second dependence of the parameters describing the RDS on γ for fixed ε has been studied earlier [38,47]. It has been emphasized that the existence of a stable RDS in CCGLE is possible due to the IRS [38]. In a recent study the role of IRS for the existence of stable propagating dissipative solitons in the CCGLE has been studied and it has been shown that the limit of the vanishing magnitude of the IRS coefficient is singular [47].

V. CCQGLE: THE INFLUENCE OF THE HIGHER-ORDER CORRECTION TERM TO THE NONLINEAR AMPLIFICATION ON THE SELF-FREQUENCY SHIFT

It is well known that the introduction of the saturation of the nonlinear gain $\mu < 0$ in CCGLE leads to the restriction of the increase of the amplitudes of solutions due to the nonlinear gain [7]. As a result of intensive numerical investigation of CCQGLE, some areas in the space of the physical parameters δ, β, ε, μ have been established, in which there have been found stable localized solutions of the CCQGLE [7]. It is shown that if $\delta < 0$, $\beta > 0$, $\varepsilon > 0$, and $\mu < 0$ the background instability is avoided [7,20]. In order to describe the properties of the self-frequency shift of RDS in the CCQGLE perturbed with IRS, we need two dependencies. The first one is the dependence of magnitudes describing the RDS on μ for fixed values of ε, γ and the second one—the dependence of magnitudes describing the RDS on γ for fixed values of ε, μ. Recently, the first dependence comparing two values of $\mu < 0$ has been studied by dynamical model [37–39] and it has been shown that the increase in the absolute value of the saturation of the nonlinear gain μ leads to the reduction of the amplitude of the high-amplitude RDS [42].

Our first aim in this section is to analyze the dependence of the parameter describing the RDS on μ for fixed values of ε, γ for a region of values of $\mu \subset [-0.1; 0]$, which allows us to discuss the properties of stationary solutions with arbitrary amplitudes. Next, we fix the value of the nonlinear gain ε and the value of the saturation of the nonlinear gain μ and change the value of parameter γ which describes the IRS. Finally, we study the properties of the RDS in the case of $\mu > 0$ fixing the values of the nonlinear gain ε and the saturation of the nonlinear gain μ and changing the value of γ.

First, we fix the value of the nonlinear gain ε and change the value of the saturation of the nonlinear gain μ in the presence of fixed IRS for $\gamma = 0.01$. A detailed comparison between the predictions of dynamic model (3) and the results obtained from the numerical simulation of Eq. (1) is presented in the next Fig. 2.

All the obtained dependencies of the magnitudes of the RDS on the value of the nonlinear gain μ presented in Fig. 2 have a monotonic character. The results presented in Fig. 2(a) clearly show that by reducing the absolute value of the saturation of the nonlinear gain μ, the amplitude of the RDS increases as should be expected from the existing singularity of solutions of CCQGLE for $\mu^- \to 0$ [13,14]. As has been mentioned, the singularity in respect to the coefficient describing the saturation of the nonlinear gain $\mu^- \to 0$ [13,14] no longer exists in the presence of IRS [42]. It is clearly seen from Fig. 2(a) that for $\mu = 0$ the peak amplitude is approximately 45.2. With the increase of the absolute value of the saturation of the nonlinear gain μ, the amplitude of the dissipative solution greatly decreases (until approximately 1 for $\mu = -0.062$), the time width increases [Fig. 2(a)], and the mean frequency steadily decreases [Fig. 2(b)]. The velocity also decreases [Fig. 2(b)]. Comparing Fig. 2(a) with Fig. 1(a), however, we can see that just contrary to the case of the nonlinear gain ε when the absolute value of its saturation increases, the amplitude of the RDS decreases and the frequency also decreases. In other words, the saturation of the nonlinear gain acts against the self-frequency shift caused by the nonlinear gain. As can be seen from Figs. 2(a) and 2(b), the predictions of dynamic model (3) for all the parameters of the RDS are in a very good agreement with the corresponding results from the numerical solution of Eq. (1).

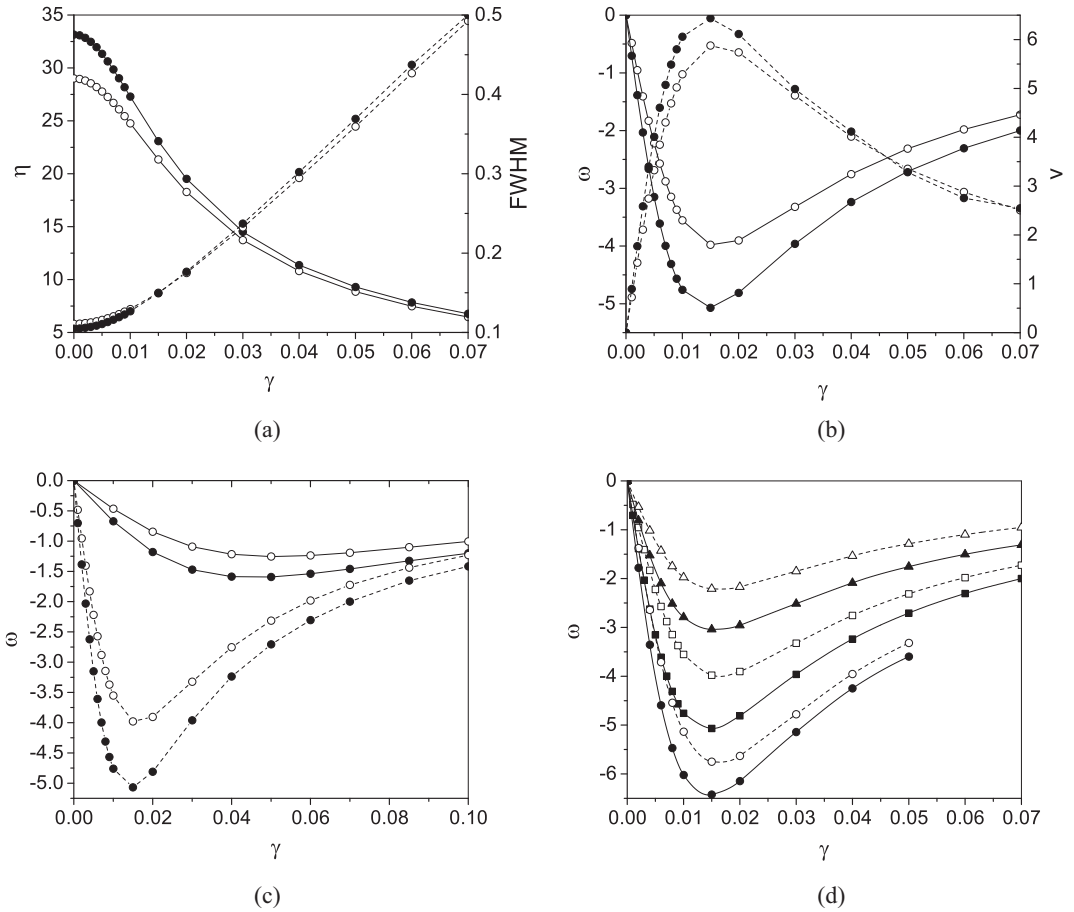

FIG. 3. Results obtained by the direct numerical solution of (1) (solid circles, triangles, squares) and the numerical solution of DM (3) (empty circles, triangles, squares) for (a) the peak amplitude (solid lines) and FWHM (dashed lines); (b) mean frequency (solid lines) and velocity (dashed lines) as functions of $\gamma \subset [0; 0.07]$ at parameters $\varepsilon = 0.3$ $\mu = -0.0001$; (c) mean frequency: $\mu = -0.001$ (solid lines) and $\mu = -0.0001$ (dashed lines) as functions of $\gamma \subset [0; 0.1]$ at parameters $\varepsilon = 0.3$; and (d) mean frequencies: $\varepsilon = 0.27$ (triangles), $\varepsilon = 0.3$ (squares), and $\varepsilon = 0.33$ (circles) as functions of γ at parameters $\mu = -0.0001$. In all cases $\delta = -0.012$; $\beta = 0.6$ and $c(0) = 0; \omega(0) = 0$

Now, we fix the value of the nonlinear gain $\varepsilon = 0.3$ and the value of the saturation of the nonlinear gain $\mu = -1 \times 10^{-4}$ and change the value of parameter γ in the range $\gamma \subset [0; 0.07]$.

As can be seen from Fig. 3(a) the dependencies of the amplitude and FWHM on γ with the increase of the value of the γ have a monotonic character: the amplitude decreases, while the pulse width increases. Due to the presence of $\mu = -1 \times 10^{-4}$, the maximum value of the amplitude decreases. In Fig. 3(b) we can observe, however, a different type of behavior of the frequency shift and the velocity of RDS as a function of γ. In fact, the frequency shift has a very well-expressed minimum (or a maximum of the absolute value of the frequency shift), while the velocity has a well-expressed maximum in the region of γ. The minimum of the frequency shift and the maximum of the velocity are for the same value of $\gamma \sim 0.015$. In other words, with the increase of the value of γ, the absolute value of the frequency at first increases until approximately $\gamma \sim 0.015$ and then the absolute value of the frequency steadily decreases. So, it turns out that we have obtained a nonlinear dependence of the absolute value of the frequency shift on γ in the presence of saturation of the nonlinear gain ($\mu = -1 \times 10^{-4}$). Obviously, the behavior of the self-frequency shift and that of velocity are related.

In Fig. 3(c) we show how the observed nonlinear dependence of the absolute value of the frequency shift on γ depends on the value of the saturation of the nonlinear gain μ. As can be seen from Fig. 3(c) with the increase of the absolute value of the saturation of the nonlinear gain up to $|\mu| = 0.001$, the maximum absolute value of the frequency shift reduces to $|\omega| \approx 1.5$ and its position moves to the larger values of $\gamma \approx 0.05$. If we further increase the absolute value of the saturation of the nonlinear gain up to $|\mu| = 0.01$, the maximum of the absolute value of the frequency shift reduces to $|\omega| \approx 0.5$ and its position moves to the larger values of $\gamma \approx 0.15$. In Fig. 3(d) we show how the observed nonlinear dependence of the absolute value of the frequency shift on γ depends on the value of the nonlinear gain ε. As can be seen from Fig. 3(d), with the increase of the value of the nonlinear gain ε, the maximum absolute value of the frequency shift increases up to $|\omega| \approx 6.5$. However, the position of its maximum does not change. For the cases studied in Fig. 3(c) and Fig. 3(d) we have observed numerically and by the dynamic model (3) the expected reduction of the amplitude of the

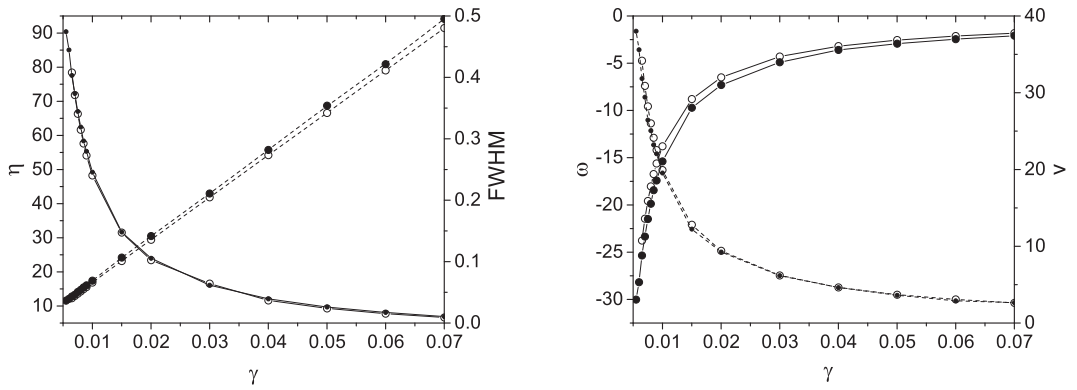

FIG. 4. Results obtained by the direct numerical solution of (1) (solid circles) and the numerical solution of DM (3) (empty circles) for (a) the peak amplitude (solid lines) and FWHM (dashed lines); (b) mean frequency (solid lines) and velocity (dashed lines) as functions of $\gamma \subset [0.0055; 0.07]$ at parameters $\delta = -0.012$; $\beta = 0.6$; $\varepsilon = 0.3$; $\mu = +3 \times 10^{-6}$.

solution with the increase of the value of γ. We have also found that, as could be expected from Fig. 1, with the increase of the value of the nonlinear gain ε the amplitudes at small γ increase. The tendency for the decrease of the amplitude with the increase the value of γ remains unchanged. (In order to maintain conciseness, these results are not presented here.) In all the examined cases, the dynamic model (3) qualitatively well describes our numerical findings.

Although the negative sign of $\mu < 0$ has a meaning of the saturation of the nonlinear gain, there have also been studied cases of $\mu > 0$ [14,16]. Here we have also studied the properties of the self-frequency shift of the RDS for positive values of μ. Figure 4 shows the evolution with γ of the parameters of RDS for fixed values of the nonlinear gain $\varepsilon = 0.3$ and of the saturation of the nonlinear gain $\mu = +3 \times 10^{-6}$.

With the increase of the value of γ, the stationary peak amplitude decreases [Fig. 4(a)], FWHM increases [Fig. 4(a)], the velocity decreases [Fig. 4(b)], and the absolute value of the frequency also decreases [Fig. 4(b)]. The dependences of all the parameters describing the RDS as a function on γ have a monotonic character. The results obtained by DM (3) are fully consistent with those obtained by Eq. (1). The results, presented in Fig. 4(b), for the dependencies of the frequency and velocity on the value of γ are very different from those shown in Fig. 3(b). The maximum absolute value of the frequency shift for small γ also increases.

We can summarize the obtained results in this section in the following way. We have observed numerically a nonlinear dependence of the self-frequency shift of RDS on the parameter γ describing IRS in the presence of the saturation of the nonlinear gain [Figs. 3(a) and 3(b)]. With the increase of the value of the saturation of the nonlinear gain, the maximum absolute value of the frequency shift decreases and its position moves to the larger values of parameter γ describing IRS [Fig. 3(c)]. The increase in the value of the nonlinear gain leads to an increase in the value of the maximum absolute value of the frequency shift, without changing its position [Fig. 3(d)]. For positive values of μ, all the parameters characterizing the dissipative solutions tend to change in a very similar way to those of the CCGLE perturbed with IRS. All the obtained numerical results are very well described by dynamic model (3).

VI. CCQGLE: THE INFLUENCE OF THE HIGHER-ORDER CORRECTION TERM TO THE NONLINEAR REFRACTIVE INDEX ON THE SELF-FREQUENCY SHIFT

In this section we will study the influence of the higher-order correction term on the nonlinear refractive index [14–16] ν on the self-frequency shift of RDS for a fixed value of the nonlinear gain. It has already been mentioned that higher-order correction terms to the nonlinear refractive index [14–16] ν when negative ($\nu < 0$) correspond to the saturation of the nonlinear refraction index [10].

Our first aim in this section is to analyze the dependence of the magnitudes describing the RDS on ν for fixed values of ε, γ for a region of values of $\nu \subset [-3 \times 10^{-5}; 0.4]$, which allows us to discuss the properties of stationary solutions with arbitrary amplitudes. Second, we will fix the value of the nonlinear gain ε and the value of the saturation of the nonlinear refractive index $\nu < 0$ and change the value of parameter γ which describes IRS. Finally, we will study the properties of the RDS in the case of $\nu > 0$ fixing the values of the nonlinear gain ε and the saturation of the nonlinear refractive index $\nu > 0$ and changing the value of γ.

First, we fix the value of nonlinear gain ε and change the value of the saturation of the nonlinear refractive index ν in the presence of fixed IRS for $\gamma = 0.01$. A detailed comparison between the predictions of dynamic model (3) and the results obtained from the numerical simulation of Eq. (1) is presented in Fig. 5 below.

In the presented region of $\nu \subset [-3 \times 10^{-5}; 0.4]$ we have found stationary solutions. All dependencies of RDS on the value of ν, presented in Fig. 5, have a monotonic character. The obtained results show that by increasing the value of the positive ν, the amplitude of the RDS decreases [Fig. 5(a)], while the FWHM increases [Fig. 5(a)]. The frequency shift and velocity greatly decrease [Fig. 5(b)]. Comparing Fig. 5(a) with Fig. 1(a), however, we can see that just opposite to the case of the nonlinear gain ε when the absolute value of the higher-order correction terms to the nonlinear refractive index

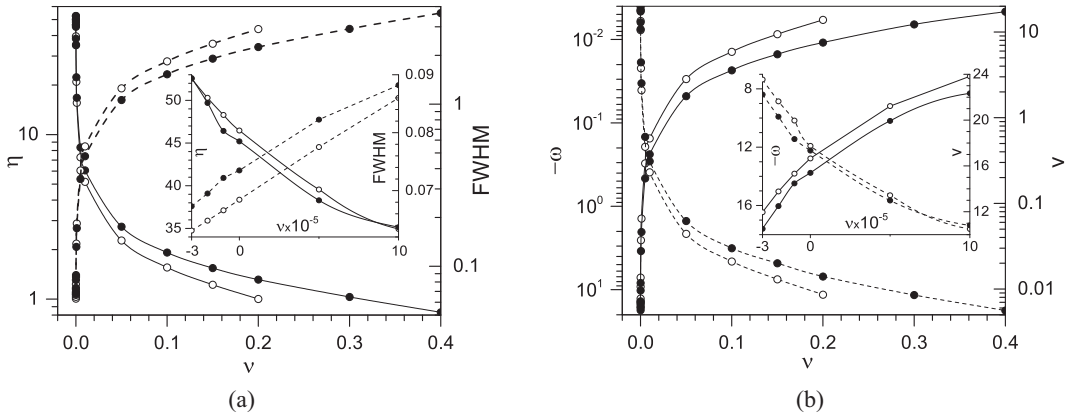

FIG. 5. Results obtained by the direct numerical solution of (1) (solid circles) and the numerical solution of DM (3) (empty circles) for (a) the peak amplitude (solid lines) and FWHM (dashed lines); (b) mean frequency (solid lines) and velocity (dashed lines) as functions of $\nu \subset [-3 \times 10^{-5}; 0.4]$ at parameters $\delta = -0.012$; $\beta = 0.6$; $\varepsilon = 0.3$; $\gamma = 0.01$.

increases, the amplitude of the dissipative solution decreases and the frequency also decreases. In other words, the higher-order correction terms to the nonlinear refractive index act against the self-frequency shift caused by the nonlinear gain. Both numerical simulations of Eq. (1) and dynamic model (3) reveal the existence of high-amplitude solutions [see Fig. 5(a)] for very small values of ν. Figure 5 also presents the results obtained for negative values of ν (internal figures). In particular, the parameters of RDS have been calculated for three values of $\nu = (-1, -2, -3) \times 10^{-5}$.

The presented results clearly show that by increasing the value of γ, the amplitude of the RDS decreases [Fig. 6(a)], while the FWHM increases [Fig. 6(a)]. The frequency shift and the velocity greatly decrease [Fig. 6(b)] and the velocity decreases. We can observe a good correlation between the results from the numerical simulations of Eq. (1) and dynamic model (3).

It has also been mentioned that we will consider the case of $\nu > 0$ studied in Refs. [14,16]. We present here our results from the study of the properties of the self-frequency shift of the RDS for positive values of ν. Figure 7 shows the evolution with γ of the parameters of RDS for a fixed value of the nonlinear gain $\varepsilon = 0.3$ and the following fixed values of the saturation of the nonlinear gain: $\nu = 0.0001$ and $\nu = 0.001$.

We should mention that the logarithmic scale on the horizontal axes in Fig. 7 is introduced for a better observation of the obtained results. Our findings from Fig. 7 are as important as those in Fig. 3. In Fig. 7(a) we can see that if we increase the value of the γ, the values of the amplitude of the RDS decrease while the pulse width increases. In Fig. 7(b) we can observe something very different in comparison with Fig. 6(b) (case for negative ν). In fact, with the increase of γ, the absolute value of the frequency of RDS increases up to approximately $\gamma \sim 0.008$. If we further increase the values of γ, however, the absolute value of the frequency steadily decreases. So, as can be seen in Fig. 7(b), it turns out that due to the presence of the higher-order correction term to the nonlinear refractive index $\nu = 0.0001$, the monotonic increase in the absolute value of the frequency shift from Fig. 2(b) is replaced by the existence of maximum absolute value of the frequency shift, after which the absolute value of the frequency shift is reduced. This nonlinear dependence of the

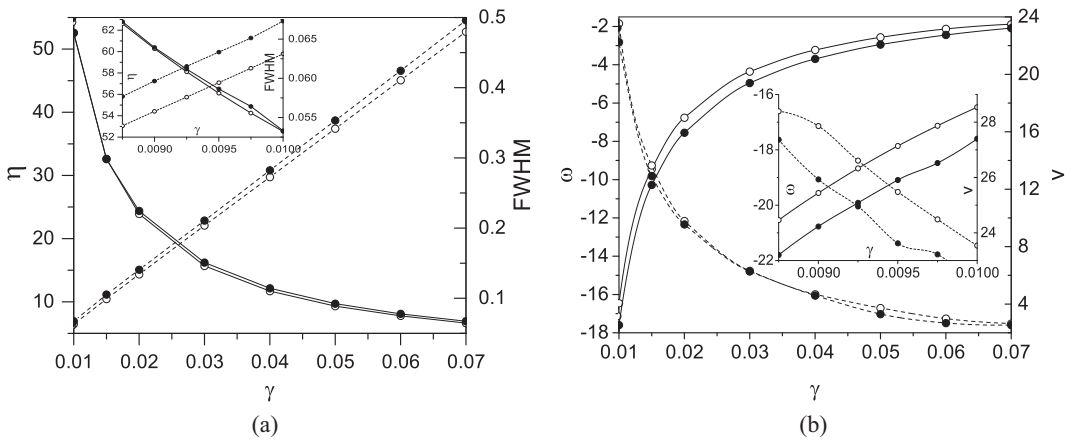

FIG. 6. Results obtained by the direct numerical solution of (1) (solid circles) and the numerical solution of DM (3) (empty circles) for (a) the peak amplitude (solid lines) and FWHM (dashed lines); (b) mean frequency (solid lines) and velocity (dashed lines) as functions of $\gamma \subset [0.008\,75; 0.07]$ at parameters $\delta = -0.012$; $\beta = 0.6$; $\varepsilon = 0.3$; $\nu = -3 \times 10^{-5}$.

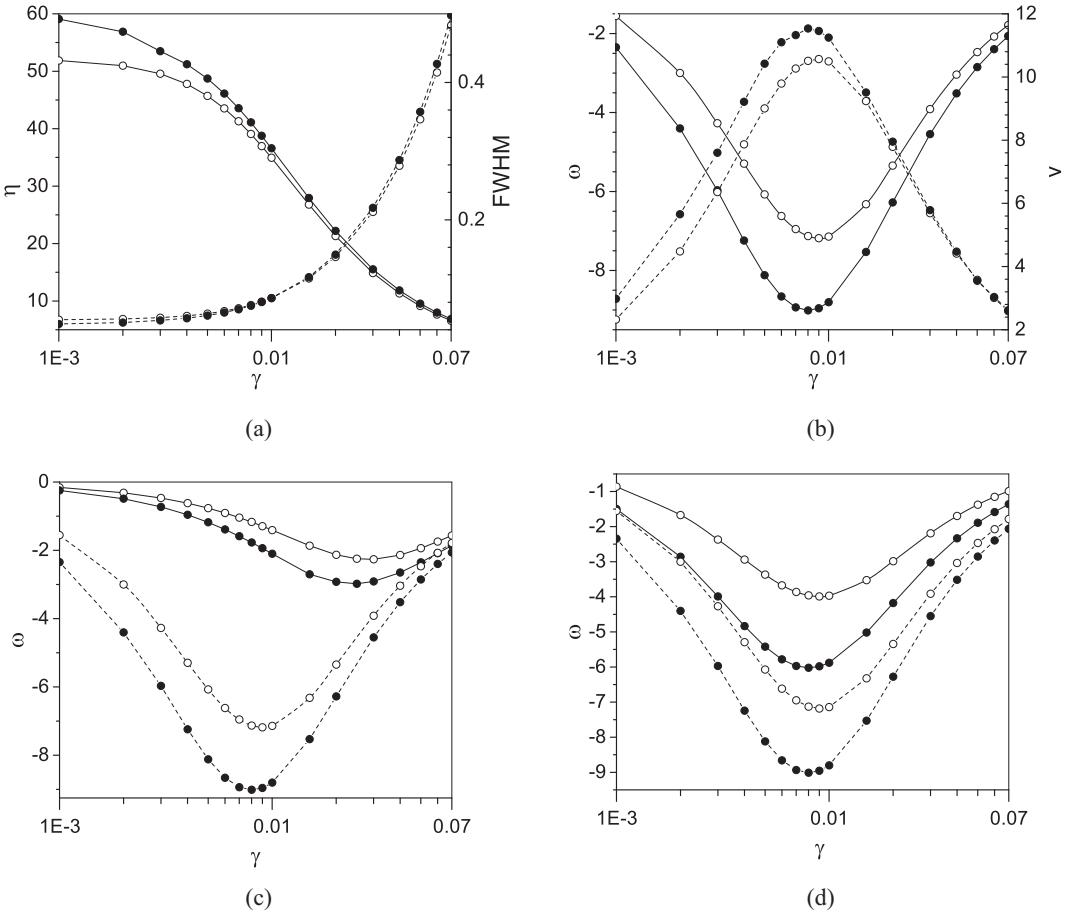

FIG. 7. Results obtained by the direct numerical solution of (1) (solid circles) and the numerical solution of DM (3) (empty circles) for (a) the peak amplitude (solid lines) and FWHM (dashed lines); (b) mean frequency (solid lines) and velocity (dashed lines) as functions of $\gamma \subset [0.001; 0.07]$ at parameters $\delta = -0.012$; $\beta = 0.6$; $\varepsilon = 0.3$; $\nu = 0.0001$; (c) mean frequency: $\nu = 0.001$ (solid lines) and $\nu = 0.0001$ (dashed lines) as functions of $\gamma \subset [0.001; 0.07]$ at parameters $\delta = -0.012$; $\beta = 0.6$; $\varepsilon = 0.3$; (d) $\varepsilon = 0.27$ (solid lines) and $\varepsilon = 0.3$ (dashed lines) as functions of γ at parameters $\delta = -0.012$; $\beta = 0.6$; $\nu = 0.0001$.

absolute value of the frequency shift on γ in the presence of the higher-order correction term to the nonlinear refractive index is a new feature of the self-induced frequency shift. The position at which the frequency reaches its minimum value (or its absolute value reaches its maximum) $\gamma \sim 0.008$ is lower than the corresponding value in Fig. 5(b) $\gamma \sim 0.015$. There is an interesting fact worth mentioning that at $\gamma = 0.07$ the calculated value of the self-frequency shift in Fig. 7(b) is comparable with that in Fig. 3(b). The nonlinear dependence of the velocity on γ can be observed in Fig. 7(b). Figure 7(c) shows how the observed nonlinear dependence of the absolute value of the frequency shift on γ depends on the value of the higher-order correction term to the nonlinear refractive index ν. As can be seen, with the increase of the value of the higher-order correction term to the nonlinear refractive index $\nu = 0.001$, the maximum absolute value of the frequency shift decreases to $|\omega| \approx 2.98$ and its position moves to larger values of $\gamma = 0.025$. We can see that the absolute value of the self-frequency shift could be reduced and controlled by increasing the value of the higher-order correction term to the nonlinear refractive index ν. Figure 7(d) shows that with the increase of the value of the nonlinear gain ε, the maximum absolute value of the frequency shift increases up to $|\omega| \approx 9$. However, the position of the maximum frequency value does not change.

We have also found that (as could be expected from Fig. 1) with the increase of the value of the nonlinear gain ε, the amplitude at small γ increases. The tendency for reduction of the amplitudes by increasing the value of γ (see Fig. 2) remains unchanged. (In order to maintain conciseness, these results are not presented here.) In all the considered cases, the dynamic model (3) qualitatively well describes the observed dependencies of the parameters describing the numerical solution.

Finally, Fig. 8 below presents two examples for the combined influence of the saturation of the nonlinear gain ($\mu < 0$) and the effect of the higher-order correction term $\nu > 0$ and $\nu < 0$ to the nonlinear refractive index [14–16] ν on the self-frequency shift of RDS.

In Fig. 8 we can observe a reduction of the maximum value of the amplitude for positive values of ν and a reduction of the maximum absolute value of the self-frequency shift. We have found that there is a growth in the maximum value of the amplitude for negative values of ν and a rise in the maximum absolute value of the self-frequency shift. In both

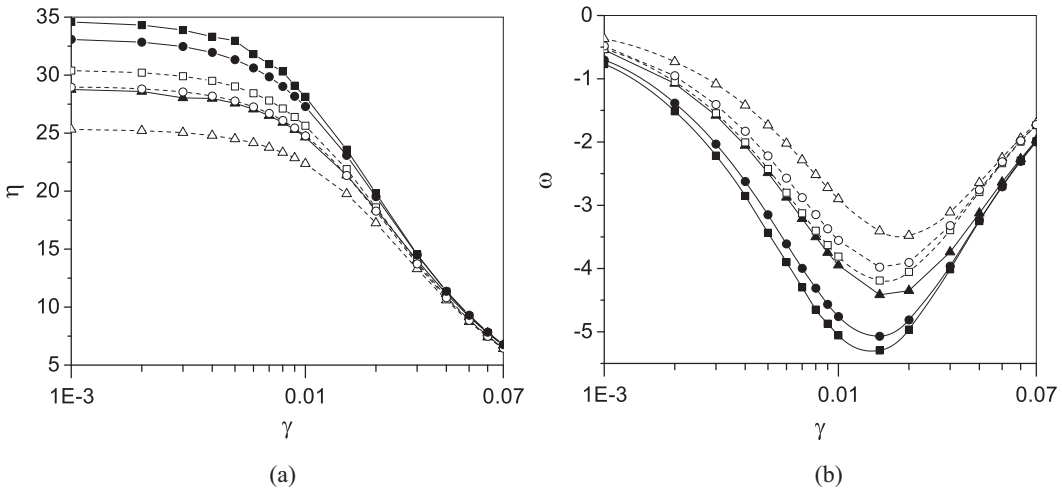

FIG. 8. Results obtained by the direct numerical solution of (1) (solid lines, solid squares, circles, or triangles) and the numerical solution of DM (3) (dashed lines, empty squares, circles, or triangles) for (a) peak amplitudes and (b) mean frequencies for the following cases: $\nu = 0$ (circles), $\nu = 0.0001$ (triangles), and $\nu = -0.000\,03$ (squares) as functions of $\gamma \subset [0.001; 0.07]$ at parameters $\delta = -0.012$; $\beta = 0.6$; $\mu = -0.0001$.

cases, however, the position of the minimum value of the self-frequency shift remains unchanged.

We can summarize the obtained results in this section in the following way. We have observed numerically the nonlinear dependence of the absolute value of the frequency shift on the parameter describing IRS in the presence of the higher-order correction term to the nonlinear refractive index [Fig. 7(b)]. With the increase of the value of the higher-order correction term to the nonlinear refractive index, the maximum absolute value of the frequency shift decreases and its position moves to larger values of parameter γ describing IRS [Fig. 7(c)]. The increase in the value of the nonlinear gain leads to an increase in the value of the maximum absolute value of the frequency shift, without changing its position [Fig. 7(d)]. In all the phenomena considered, a very good agreement has been identified between the results obtained by the numerical solution of Eq. (1) and dynamic model (3) [44]. In the case of the combined influence of the saturation of the nonlinear gain $\mu < 0$ and the effect of the higher-order correction term to the nonlinear refractive index $\nu > 0$, there has been found a reduction of the maximum absolute value of self-frequency shift.

VII. PERFORMANCE OF THE DYNAMIC MODEL

Our study presents material for discussion of the usefulness of finite-dimensional dynamic models in the study of systems with infinite number of degrees of freedom. First, we would like to mention that the complete dynamic model of [44] describes the CCQGLE perturbed with IRS, TOD, and SS. Here we use the particular cases of the model for CCGLE perturbed with IRS in Sec. IV and for the CCQGLE perturbed with IRS in Secs. V and VI. In the case of the perturbed with IRS CCGLE discussed in Sec. IV, there have been found approximate fixed points. We believe that it has been clearly shown in Secs. IV–VI that at least in the regions of the values of the parameters discussed here, dynamic model (3) provides reasonable results for all the parameters of the sech-like RDS in all the considered phenomena. The main reason for the observed good agreement between the results obtained by the direct numerical solution of Eq. (1) and those obtained by dynamic model (3) is the preservation of the sech-like form of numerical solutions, which we have established in the process of our study. The reason for the observed preservation of the sech-like time shape of the numerical solutions is related to the relatively small values of the nonlinear gain ε. As is well known for large values of the nonlinear gain ε, there exists a variety of new numerical solutions of the CCQGLE [9,10]. The application of the dynamic model (3) has helped us in the obtaining of the proper initial conditions for the numerical analysis and allowed us to save computational time for the numerical simulations. Our study has also made it clear that the dynamic model of Ref. [44] performs better than that of Refs. [37–40]. An interesting question remains open: whether the alternative dynamic model applied as ansatz function and connected to the exact solution of the CCQGLE could lead to more accurate results than those obtained here.

VIII. CONCLUSIONS

In this work we have presented a study of the influence of the nonlinear gain (absorption), the influence of higher-order correction terms to the nonlinear amplification (absorption), and the influence of higher-order correction terms to the nonlinear refractive index on the self-frequency shift of Raman dissipative solitons. In order to accomplish this aim, we have applied two methods: the numerical solution of the basic equation with the help of Agrawal's split-step Fourier method with two iterations [58], and the dynamic model obtained with the method of moments [44].

We have shown that with the increase of the value of the nonlinear gain ε, the pulses increase their amplitude and reduce their width, i.e., solutions compress. There is an increase in the frequency and the velocity of the Raman dissipative solitons.

We have observed numerically a nonlinear dependence of the self-frequency shift of Raman dissipative solitons on the parameter γ describing IRS in the presence of the saturation of the nonlinear gain. With the increase of the value of the saturation of the nonlinear gain, the maximum absolute value of the frequency shift decreases and its position moves to larger values of parameter γ describing IRS. The increase in the value of the nonlinear gain leads to an increase in the maximum absolute value of the frequency shift, without changing its position. We have also observed numerically the nonlinear dependence of the absolute value of the frequency shift on the parameter describing IRS in the presence of the higher-order correction term to the nonlinear refractive index. With the increase of the value of the higher-order correction term to the nonlinear refractive index, the maximum absolute value of the frequency shift decreases and its position moves to larger values of parameter γ describing IRS. The increase in the value of the nonlinear gain leads to an increase in the maximum absolute value of the frequency shift, without changing its position. In all the considered phenomena, a very good agreement has been identified between the results obtained by the numerical solution of Eq. (1) and those of dynamic model (3) of Ref. [44]. In the case of the combined influence of the saturation of the nonlinear gain $\mu < 0$ and the effect of the higher-order correction term to the nonlinear refractive index $\nu > 0$, a reduction in the maximum absolute value of the self-frequency shift has been found.

We can conclude that the observed nonlinear dependences of the self-frequency shift on the value of the saturation of the nonlinear gain as well as on the value of the higher-order correction term to the nonlinear refractive index can be used for the better understanding and control of the spectral characteristics of Raman dissipative solitons.

The influence of the other higher-order effects as well as the noise on the phenomena observed here could be the topics of further studies.

[1] H. A. Haus, J. Appl. Phys. **46**, 3049 (1975).
[2] H. A. Haus, J. G. Fujimoto, and E. P. Ippen, J. Opt. Soc. Am. B **8**, 2068 (1991).
[3] J. D. Moores, Opt. Commun. **96**, 65 (1993).
[4] M. Matsumoto, H. Ikeda, T. Uda, and A. Hasegawa, J. Lightwave Technol. **13**, 658 (1995).
[5] A. Hasegawa and Y. Kodama, *Solitons in Optical Communications* (Clarendon, Oxford, 1995).
[6] G. P. Agrawal, *Applications of Nonlinear Fibre Optics* (Academic Press, San Diego, CA, 2001).
[7] N. N. Akhmediev and A. Ankiewicz, *Solitons: Nonlinear Pulses and Beam* (Chapman and Hall, London, 1997).
[8] N. N. Akhmediev and A. Ankiewicz, in *Dissipative Solitons*, edited by N. N. Akhmediev and A. Ankiewicz, Lecture Notes in Physics, Vol. 661 (Springer, Berlin, 2005).
[9] J. M. Soto-Crespo, N. Akhmediev, and A. Ankiewicz, Phys. Rev. Lett. **85**, 2937 (2000).
[10] N. N. Akhmediev, J. M. Soto-Crespo, and G. Town, Phys. Rev. E **63**, 056602 (2001).
[11] W. van Saarloos and P. C. Hohenberg, Phys. Rev. Lett. **64**, 749 (1990).
[12] N. N. Akhmediev and V. V. Afanasjev, Phys. Rev. Lett. **75**, 2320 (1995).
[13] V. V. Afanasjev, Opt. Lett. **20**, 704 (1995).
[14] N. N. Akhmediev, V. V. Afanasjev, and J. M. Soto-Crespo, Phys. Rev. E **53**, 1190 (1996).
[15] V. V. Afanasjev, N. N. Akhmediev, and J. M. Soto-Crespo, Phys. Rev. E **53**, 1931 (1996).
[16] J. M. Soto-Crespo, N. N. Akhmediev, and V. V. Afanasjev, J. Opt. Soc. Am. B **13**, 1439 (1996).
[17] J. M. Soto-Crespo, N. N. Akhmediev, and G. Town, Opt. Commun. **199**, 283 (2001).
[18] A. I. Maimistov, J. Exp. Theor. Phys. **77**, 727 (1993); Zh. Eksp. Teor. Fiz. **104**, 3620 (1993) (in Russian).
[19] E. Tsoy and N. N. Akhmediev, Phys. Lett. A **343**, 417 (2005).
[20] E. Tsoy, A. Ankiewicz, and N. Akhmediev, Phys. Rev. E **73**, 036621 (2006).
[21] M. V. Kozlov, C. J. McKinstrie, and C. Xie, Opt. Commun. **251**, 194 (2005).
[22] S. C. Mancas and S. R. Choudhury, Chaos, Solitons Fractals **40**, 91 (2009).
[23] Z. Li, L. Li, H. Tian, G. Zhou, and K. H. Spatschek, Phys. Rev. Lett. **89**, 263901 (2002).
[24] L. Song, L. Li, Z. Li, and G. Zhou, Opt. Commun. **249**, 301 (2005).
[25] P.-A. Bélanger, Opt. Express **14**, 12174 (2006).
[26] E. M. Dianov, A. Ya. Karasik, P. V. Mamyshev, A. M. Prokhorov, V. N. Serkin, M. F. Stel'makh, and A. A. Fomichev, JETP Lett. **41**, 294 (1985).
[27] F. M. Mitschke and L. F. Mollenauer, Opt. Lett. **11**, 659 (1986).
[28] V. N. Serkin, Sov. Tech. Phys. Lett. **13**, 320 (1987).
[29] J. M. Dudley, G. Genty, and S. Coen, Rev. Mod. Phys. **78**, 1135 (2006).
[30] A. M. Zheltikov, Phys.-Usp. **54**, 29 (2011).
[31] S. C. Latas, M. F. S. Ferreira, and M. Facao, Appl. Phys. B **104**, 131 (2011).
[32] S. C. Latas and M. F. S. Ferreira, Opt. Lett. **36**, 3085 (2011).
[33] M. V. Facao and M. I. Carvalho, Phys. Lett. A **376**, 950 (2012).
[34] C. Cartes and O. Descalzi, Eur. Phys. J. Spec. Top. **223**, 91 (2014).
[35] C. Cartes and O. Descalzi, Fiber Integr. Opt. **34**, 14 (2015).
[36] O. Descalzi and C. Cartes, Appl. Sci. **7**, 887 (2017).
[37] H. Tian, Z. Li, Z. Hu, J. Tian, and G. Zhou, J. Opt. Soc. Am. B **20**, 59 (2003).
[38] S. C. V. Latas and M. F. S. Ferreira, Opt. Commun. **251**, 415 (2005).
[39] I. M. Uzunov, Z. D. Georgiev, and T. N. Arabadzhiev, Phys. Rev. E **90**, 042906 (2014).
[40] I. M. Uzunov, T. N. Arabadzhiev, and Z. D. Georgiev, Proc. SPIE **9447**, 94471G (2015).
[41] I. M. Uzunov, Z. D. Georgiev, and T. N. Arabadzhiev, Phys. Rev. E **97**, 052215 (2018).
[42] S. C. Latas, M. F. S. Ferreira, and M. Facao, J. Opt. Soc. Am. B, **34**, 1033 (2017).
[43] A. Sahoo, S. Roy, and G. P. Agrawal, Phys. Rev. A **96**, 013838 (2017).
[44] I. M. Uzunov, T. N. Arabadzhiev, and Z. D. Georgiev, Opt. Fiber Technol. **24**, 15 (2015).

[45] A. Ankiewicz, M. Bokaeeyan, and N. Akhmediev, J. Opt. Soc. Am. B **35**, 899 (2018).
[46] I. M. Uzunov and T. N. Arabadzhiev, Appl. Phys. B **125**, 221 (2019).
[47] O. Descalzi, J. Cisternas, and H. R. Brand, Phys. Rev. E **100**, 052218 (2019).
[48] I. M. Uzunov and S. G. Nikolov, J. Mod. Opt. **67**, 606 (2020).
[49] I. M. Uzunov and T. N. Arabadzhiev, Phys. Wave Phenom. **28**, 338 (2020) (in press).
[50] I. M. Uzunov and S. G. Nikolov, Physics days 2020, Collection of popular and scientific reports, 10, 73-79, Technical University of Sofia.
[51] R. H. Stolen, J. P. Gordon, W. J. Tomlinson, and H. A. Haus, J. Opt. Soc. Am. B **6**, 1159 (1989).
[52] V. V. Afanasyev, V. A. Vysloukh, and V. N. Serkin, Opt. Lett. **15**, 489 (1990).
[53] V. N. Serkin, T. L. Belyaeva, G. H. Corro, and M. A Granados, Kvantovaya Elektron. **33**, 325 (2003).
[54] M. Erkinalo, G. Genty, B. Wetzel, and J. M. Dudley, Opt. Express **18**, 25449 (2010).
[55] F. W. Wise, A. Chong, and W. H. Renninger, Laser Photon Rev. **2**, 58 (2008).
[56] V. L. Kalashnikov and A. Apolonski, Phys. Rev. A **79**, 043829 (2009).
[57] A. Komarov, H. Leblond, and F. Sanchez, Phys. Rev. E **72**, 025604 (2005).
[58] M. J. Potasek, G. P. Agrawal, and S. C. Pinault, J. Opt. Soc. Am. B **3**, 205 (1986).
[59] I. M. Uzunov and T. N. Arabadzhiev, Opt. Quant. Electron. **51**, 283 (2019).
[60] Wolfram Mathematica 8, 2010 Wolfram Research, Inc.
[61] K. J. Blow, N. J. Doran, and D. Wood, J. Opt. Soc. Am. B, **5**, 1301 (1988).
[62] M. Nakazawa, K. Kurokawa, H. Kubota, and E. Yamada, Phys. Rev. Lett. **65**, 1881 (1990).
[63] V. V. Afanasiev, V. N. Serkin, and V. A. Vysloukh, Sov. Lightwave Commun. **2**, 35 (1992).
[64] M. F. S. Ferreira, Opt. Commun. **107**, 365 (1994).
[65] I. M. Uzunov, Phys. Rev. E **82**, 066603 (2010).